Three Dimensional Model of Oxygen Transport in a Porous Diffuser of a PEM Fuel Cell

K. V. Zhukovsky
ERG-TEA, S.P.99, ENEA-Centro Ricerche Casaccia, 00060-S.Maria di Galeria, Rome, Italy

Binary molecular diffusion and pressure-driven fluxes of gas in porous media are studied. A 2-dimensional model of gas transport in porous media is developed in the field of nonzero gradients of pressure and concentration. Spatial distributions of oxygen concentration and fluxes in a porous diffuser are analyzed for geometric and physical parameters of the electrode. A three-dimensional generalization of the model is performed. Application to oxygen-flow modeling in electrodes of polymer electrolyte fuel cells (PEFC) is discussed for two simple configurations of gas supply channels: serpentine and interdigitated. Comparison of the results obtained for the two configurations is carried out. Oxygen flux through the catalytic membrane plane is investigated for physical characteristics of gases and the diffuser, geometry of the gas supply channels, and gas pressure in them. Recommendations for an optimal pressure regime for the specific geometry of the system and its physical characteristics are given.

Introduction

Polymer electrolyte fuel cells (PEFC) represent an increasingly popular alternative source of energy. However, fuel cells with high-power densities must be developed for this technology to become a viable power source for transportation applications. Three main factors limiting the current and leading to voltage losses in proton-conducting membrane fuel cells are the following: activation resistance, attributed to the catalyst layer in contact with the electrode and accessible by the reacting gases (Amphlett et al., 1995; Bernardi, 1990; Bernardi and Verbrugge, 1991, 1992), ohmic voltage losses, attributed to the electronic, ionic, and contact resistance of the cell (Bird et al., 1960; Fuller and Newman, 1993; Gurau et al., 2000; He et al., 2000; Kumar et al., 1995), and the mass-transport resistance, when the reactant gases deplete on the reaction interface as their transport to the reaction sites fails to keep up with the reaction rate. The last phenomenon, present in particular on the cathode, still has not been fully addressed by researchers. The only common method to overcome such transport limitations and to increase the power density has been to use pressured reactants.

So far, numerous theoretical models of PEFC have been developed (see, for example, Nguyen, 1996; Nguyen and White, 1993; Perry et al., 1998; Ralph et al., 1997; Rho et al., 1998; Springer et al., 1991, 1996; Taylor, 1992). However, they are usually restricted to simple one-dimensional cases. Recent experimental studies demonstrated the significant influence of final pressure drops and geometry of supply channels on the effectiveness of the cell (Todu et al., 1998; Wainright et al., 1995; Watanabe et al., 1993; White, 1991). For example, so-called interdigitated configuration of supply channels (see Figure 1b) essentially makes use of a new pressure-driven mechanism of mass transport that acts in addition to common molecular diffusion.

This mechanism also strongly contributes to the gas transport in the electrode with a serpentine channel design (see Figure 1a) when the matter is highly porous and there are noticeable pressure gradients. By forcing the gas to flow into the electrodes in addition to flowing under their surface, the transport of the reactant and product gases to and from the catalyst layers is converted from a pure molecular diffusion process to forced convection. It also helps removing liquid water from the gas diffuser.

The aim of these studies is the development of an analytical three-dimensional model of the physical processes of gas

Dr. Zhukovksy is on a leave of absence from Moscow State University, Physical Faculty, Moscow, Russia.

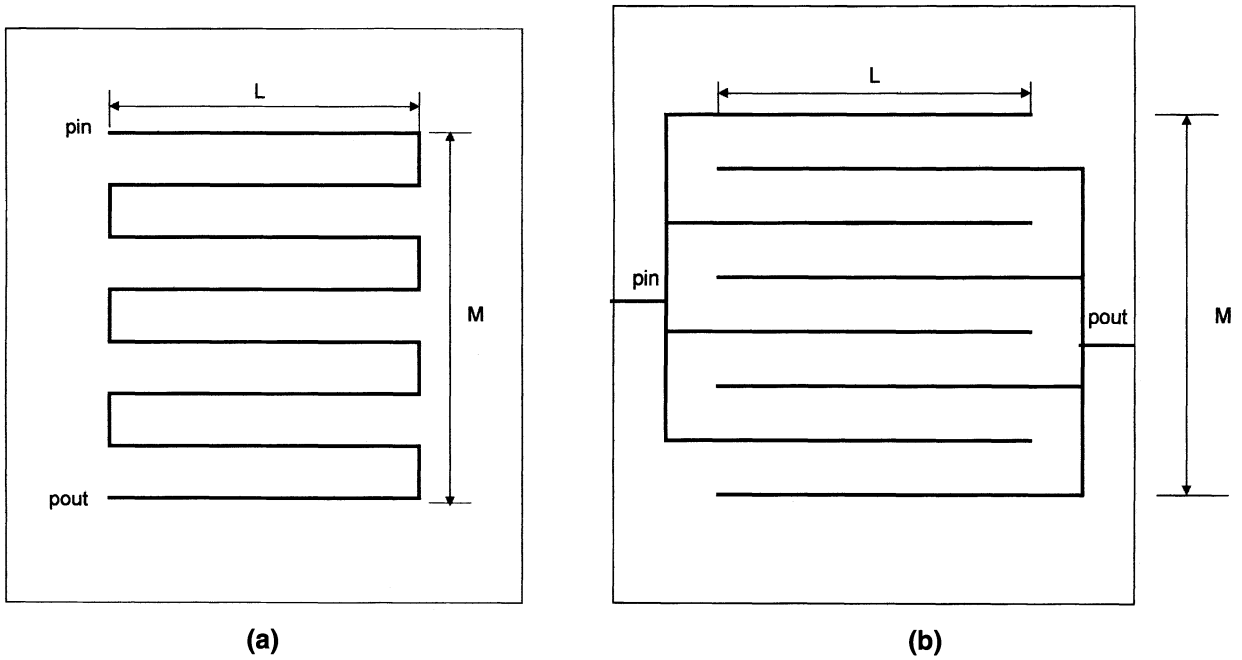

Figure 1. (a) Serpentine and (b) interdigitated configurations of gas supply channels in a polymer electrolyte fuel cell.

transport in porous media and its application to the studies of diffusion processes in the electrodes of polymer fuel cells. Expressed by functions rather than sets of numbers, analytical solutions permit the use of functional analysis to identify trends for particular uses. In the present work, we do not consider the possibility of large excesses of liquid water within the electrode. This phenomenon will be addressed in forthcoming articles, for example, on modeling a multilayered diffuser with different effective porosity-tortuosity coefficients in each layer.

A simple 3-dimensional model of gas transport in porous media, developed in the present article, accounts for gas flow in porous media in a nonzero gradient pressure field together with molecular diffusion. Application of the research includes studies of oxygen flows in diffuser and catalytic membrane over particular geometric configurations of the gas supply channels of PEFC, that is, serpentine and interdigitated (Figure 1a and 1b). The model provides a qualitative description of the physical behavior of the cell as a function of the physical characteristics of the gases and diffuser; configuration of the gas supply channels; the pressure and reactants concentration in the channels; and pressure drop. The model shows the ways to reduce the mass-transport losses and improve the performance of the polymer electrolyte fuel cell by optimizing the physical and geometric characteristics of fuel cell electrodes.

Mathematical model

We assume that the gas mixtures in the diffuser act as ideal gases, the temperature gradients are negligible ($T = const$), and the processes are steady state, no sinks and sources are present in the body of the diffuser, and the electrochemical reaction takes place on the surface of the catalytic membrane only (Figure 2). Then the fluxes of gases A and B in the body of the electrode are governed by well-known equations of diffusion, continuity equations, and D'Arcy flow equation

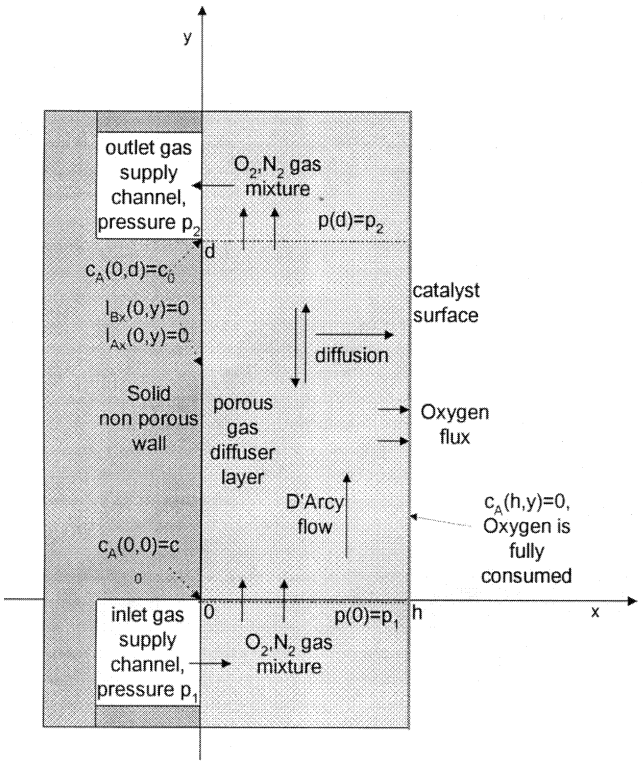

Figure 2. An electrode of a polymer electrolyte fuel cell.

(Wilson and Gottesfeld)

$$\boldsymbol{I}_i = -\rho D_{i-j}\nabla c_A + g\,\rho_i \mathbf{u}, \qquad \nabla \boldsymbol{I}_i = 0, \qquad \boldsymbol{u} = -\frac{k}{\mu}\nabla p;$$

$$i = A,B, \qquad j = B,A,$$

$$c_A + c_B = 1, \qquad c_A = \rho_A/\rho, \qquad c_B = \rho_B/\rho, \qquad p = \rho RT, \tag{1}$$

where $\boldsymbol{I}_A$, $\boldsymbol{I}_B$ are the fluxes of the gases A and B; $c_{A,B}$ are their concentrations; $\rho_{A,B}$ are their densities; ρ is total density; p is the pressure; D_{A-B}, D_{B-A} are the diffusion coefficients, $D_{A-B} = D_{B-A}$; $\boldsymbol{u}$ is the bulk speed of the gas mixture; R is the gas constant; T is the temperature; k is the permeability coefficient; and μ is the viscosity coefficient.

Usually, gas pressures at the anode and cathode of PEFC are approximately equal to each other. Then the assumption $p = p(y)$, $p(x) = \text{const}$ is justified. In order to address oxygen transport limitations, gas A (for example, oxygen) of initial concentration c_0 is considered to be fully converted on the catalyst surface of PEFC. Boundary conditions in such case of limiting current read as follows (see Figure 2)

$$p(0) = p_1, \qquad p(d) = p_2, \qquad c_A(h, y) = 0,$$

$$c_A(0,0) = c_0, \qquad c_A(0,d) = c_1,$$

$$I_{A,x}(x = 0, y) = 0, \qquad I_{B,x}(x = 0, y) = 0 \tag{2}$$

Diffusion coefficient D_{AB} is a function of temperature, pressure, and gas composition. The effective oxygen diffusion coefficient in the nitrogen–water vapor gas mixture can be calculated as a function of binary diffusion coefficients, taken from the estimation of Slattery and Bird (Yi and Nguyen, 1998). With oxygen concentration varying from 0 in the catalyst layer to the maximum possible value in saturated humid air, the change in the density–diffusivity product, ρD_{O_2} is negligible (less than 4%) under normal fuel cell operation conditions (Toda et al., 1998). Then at low pressures and constant temperature the following combinations of variables are constants

$$\alpha = pD_{AB}/RT = \text{const}, \qquad \beta = k/\mu RT = \text{const} \tag{3}$$

Then the preceding set of equations (Eqs. 1) with boundary conditions (Eqs. 2) possesses a simple analytical solution for the concentration $c_A(x,y)$ (Figure 3)

$$c_A(x, y) = \cos Fx\left(E_1 \exp\frac{H-G}{2}y + E_2 \exp\frac{H+G}{2}y\right),$$

$$E_1 = \frac{c_0 - c_1 \exp\left\{-\dfrac{G+H}{2}d\right\}}{1-\exp\{-Gd\}},$$

$$E_2 = \frac{-c_0 \exp\{-Gd\} + c_1 \exp\left\{-\dfrac{G+H}{2}d\right\}}{1-\exp\{-Gd\}}, \tag{4}$$

$$G = \sqrt{4F^2 + H^2}, \qquad F = \frac{\pi}{2h}, \qquad H = -\frac{\beta}{\alpha}\frac{p_2^2 - p_1^2}{2d}$$

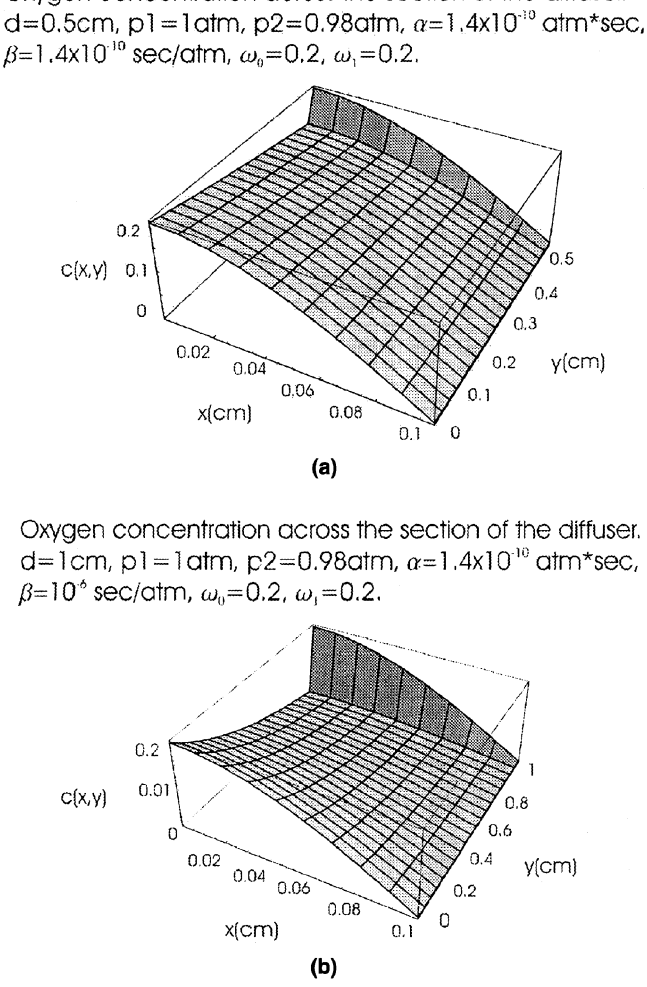

Figure 3. Concentration profile $c(x,y)$ of oxygen, diffusing nitrogen in 0.1-cm-thick porous diffuser with permeability $k = 1.6\times10^{-7}$ cm^2 over two channels pressured at $p_1 = 10^5$ Pa, $p_2 = 9.8\times10^4$ Pa, and distant at (a) $d = 0.5$ cm, (b) $d = 1.0$ cm. (See also Figure 2).

Here p_1, p_2 are the pressures in the two points of the two channels in question, d is the distance between those points, h is the thickness of the diffusive layer, c_0 is the initial concentration of substance A in the "in" channel, c_1 is the final concentration of substance A in the "out" channel, α and β are given by Eq. 3.

The expressions (Eqs. 4) for the concentration yield the flux through the membrane J_A (Figure 4) as follows

$$J_A = \int_0^d j_{Ax}(h,y)\,dy = \alpha\frac{\pi}{h}\left(\frac{E_1}{H-G}\exp\frac{H-G}{2}y + \frac{E_2}{H+G}\exp\frac{H+G}{2}y\right) \tag{5}$$

For oxygen as A gas, membrane flux J_{O_2} increases in the vicinity of the channels at $y = 0$ and $y = d$.

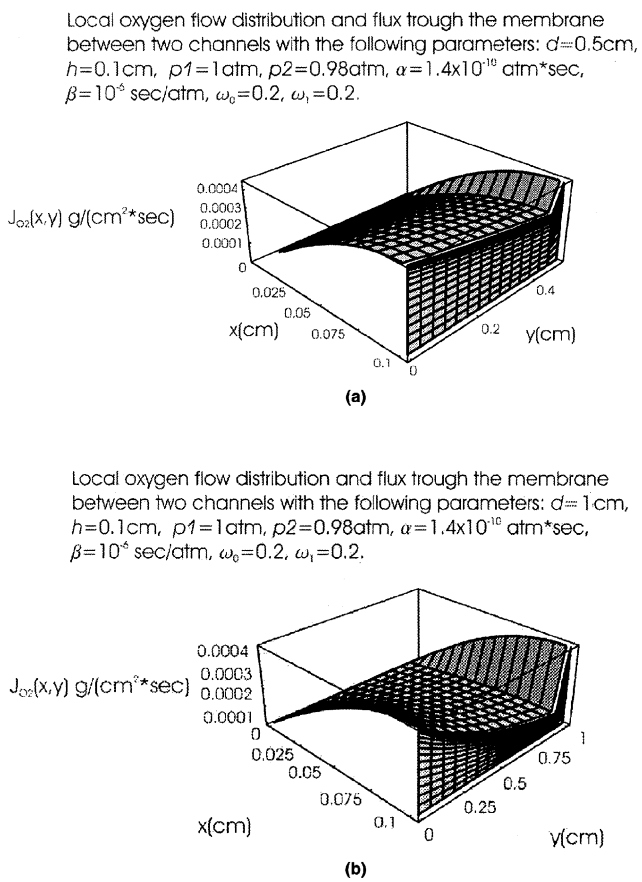

Figure 4. Catalyst-directed oxygen flow distribution $j_{Ax}(x,y)$ across the section of diffuser between two channels, distant at (a) $d = 0.5$ cm, (b) 1.0 cm at the set conditions just given (see Figure 1) and oxygen flux J_{O_2} through the catalyst line $x = h$—the vertical shadows on the right side of the picture boxes.

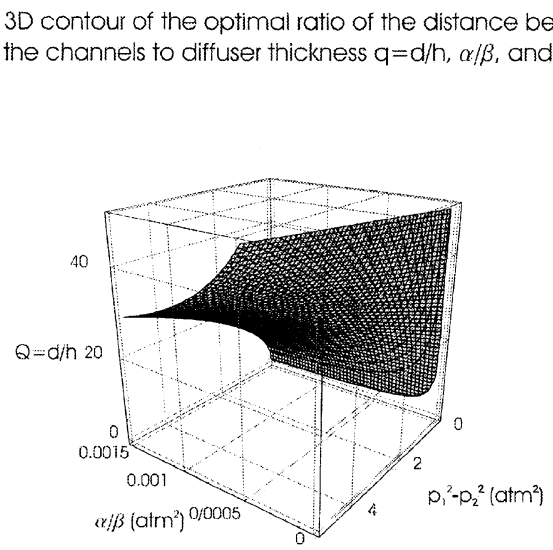

Figure 5. Maximum flow 3-D contour, relating the ratio of optimal height of the diffusive layer to the distance between the neighboring channels, average pressures in the channels, and physical characteristics of the gases and diffuser.

For the case of the two parallel channels at $y = 0$ and $y = d$, the oxygen flux per unit of channel length through the catalyst surface J_{O_2} is at its maximum, determined by the transcendental function of the ratio d/h of the distance between the two channels to the diffuser thickness, as well as of the physical parameters ratio α/β and the difference $p_1^2 - p_2^2$ (Figure 5). For $h = 0.1$ cm, $k = 1.6\times10^{-7}$ cm^2, $p_1 = 10^5$ Pa, $p_2 = 9.8\times10^4$ Pa, $J_{O_2}[d = \{0.5,\ 1.0,\ 1.5,\ 2.0\}_{cm}] = \{1.8\times10^{-5},\ 2.1\times10^{-5},\ 1.7\times10^{-5},\ 1.4\times10^{-5}\}$kg/(m·s). The diffuser with permeability $k \sim 10^{-7} - 10^{-8}$ cm^2 and $p_1 = 10^5$ Pa, $\delta p = 2\times10^3$ Pa transports oxygen to the membrane most effectively when the ratio $q \sim 5$–10.

When pressure and its drop are sufficiently high, that is, $p_1^2 - p_2^2 \gtrsim 2\pi q(\alpha/\beta)$, $q = d/h$, D'Arcy flow dominates over diffusion in the y-direction. The asymptote of the catalyst oxygen flux, J_{O_2}, at high pressures and drops, that is, $p_1^2 - p_2^2 \gg q^2(\alpha/\beta)$, is independent of pressure, its drop, and permeability, as the diffuser is saturated with oxygen. At lower pressures, that is, $2\pi q(\alpha/\beta) < p_1^2 - p_2^2 < q^2\ (\alpha/\beta)$ the flux J_{O_2} is proportional to $p_1^2 - p_2^2$, but it is independent of the diffusion coefficient. Note that the flux appears to depend on the dimensionless ratio q, but not on the geometric sizes d and h. When $p_1^2 - p_2^2 \lesssim 2\pi q(\alpha/\beta)$, oxygen is transported by diffusion alone.

Three-Dimensional Generalization of the Model

Suppose parameters d, $p_{1,2}$, $c_{0,1i}$ are not constants, but rather are functions of variable z

$$d = d(z), \qquad c_0 = c_0(z), \qquad c_1 = c_1(z), \qquad p_1 = p_1(z), \qquad p_2 = p_2(z) \quad (6)$$

In reality, the length of the gas-supply channel, L, in PEFC is greater than the distance between them, d, and the diffuser thickness, h: $L \gg d$, $L \gg h$. Then the following relations $\partial p/\partial y \gg \partial p/\partial z$, $\nabla p|\ |y$ hold everywhere in the closed-channel net (Figure 1a), but not for the vicinity of the turn points in the continuous channel net (Figure 1b). The contribution of the latter is small, because of the low pressure drop between neighboring channels at the turning points. Consequently, gas fluxes in the diffuser, directed along the supply channels, are negligible respectively to those across the diffuser. The substance A, for example, oxygen on the cathode, the flux through the membrane at $x = h$ over two neighboring channels, becomes

$$\Omega_A = \alpha\frac{\pi}{h}\int dz\left(\frac{E_1(z)}{H(z)-G(z)}\exp\frac{H(z)-G(z)}{2}y + \frac{E_2(z)}{H(z)+G(z)}\exp\frac{H(z)+G(z)}{2}y\right), \quad (7)$$

where E_1, E_2, G, H, F are given by Eqs. 4 with account for Eq. 6; $p_1(z)$, $c_0(z)$ are the inlet channel pressure and oxygen concentration; $p_2(z)$, $c_1(z)$ are the outlet channel pressure and oxygen concentration, respectively; and α and β are constants, given by Eqs. 3.

Application to Certain Configurations of Electrodes of Polymer Fuel Cells

Consider two common configurations that are parallel to each other, equidistant, and are channels in the electrode: a net of channels of continuous design (Fig.1a) and so-called interdigitated design (Figure 1b).

Interdigitated design

An interdigitated design employs only two kinds of separate channels, that is, *in* and *out*. Suppose the oxygen concentration along the channels is maintained constant and equal to concentrations $c_{0,1}$ (generally speaking, oxygen depletes along the channels if there is no forced flow in it, so that the average values $c_{0,1i}$ may be lower than the concentrations $c_{0,1}$). Then the oxygen flux through the membrane at $x = h$ over the plate of interdigitated channels can be written as follows (Figure 6)

$$\Omega_{\text{int,dig}} = (n-1)\pi\alpha\frac{L}{h}\left(\frac{E_1}{H-G}\exp\frac{H-G}{2}y + \frac{E_2}{H+G}\exp\frac{H+G}{2}y\right) \quad (8)$$

where E_1, E_2, G, H, F are given by Eqs. 4; α, β are given by Eqs. 5; $d = M/(n-1)$; n is the number of channels; M is the width of the channel plate; L is the single channel length; p_1

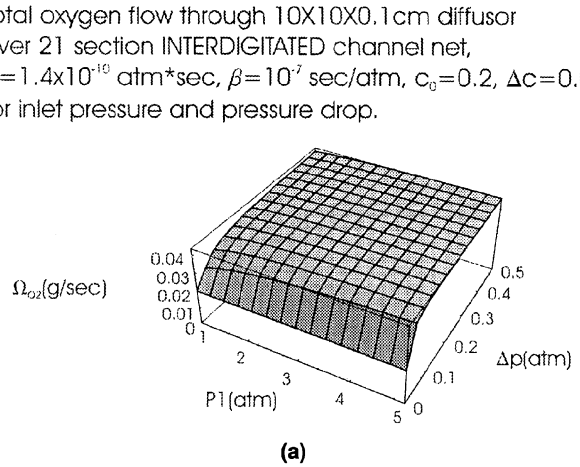

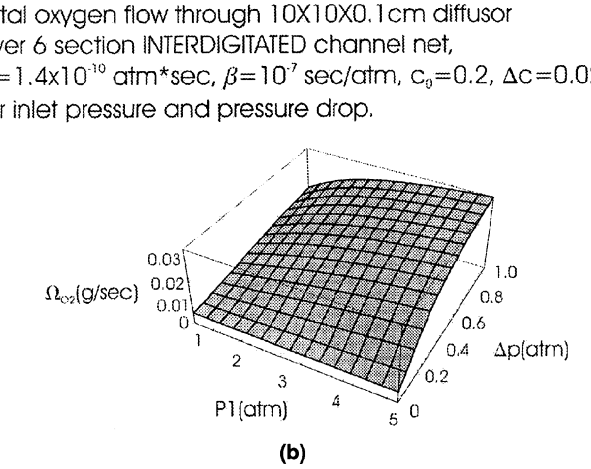

Figure 6. The oxygen flows through the membrane plane $x = h$ over 21- and 6-section interdigitated channels and 1-mm-thick diffuser with permeability $k = 1.6 \times 10^{-8}$ cm^2 in the regime of full conversion of oxygen on the membrane for inlet pressure p_1 and pressure drop ΔP.

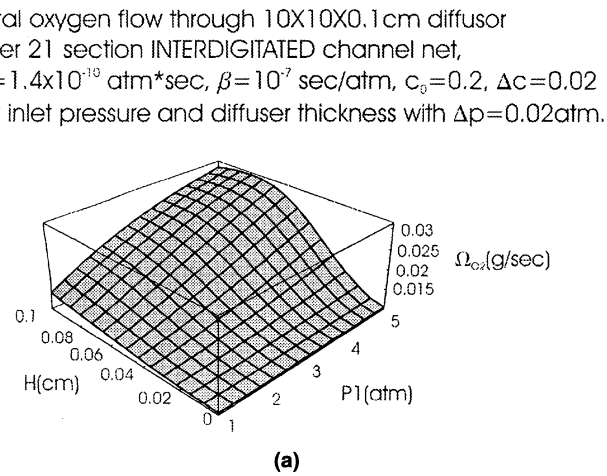

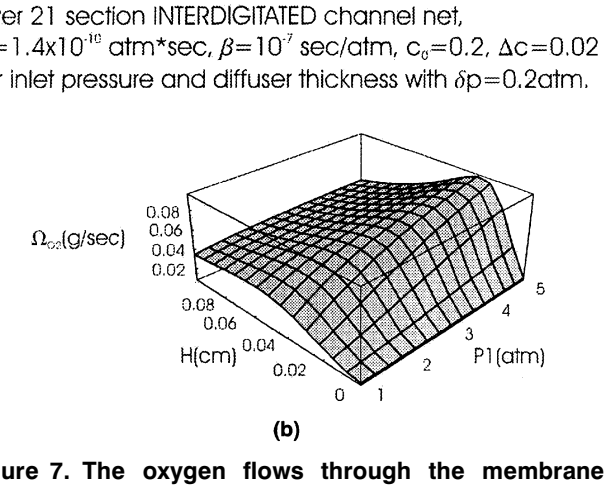

Figure 7. The oxygen flows through the membrane plane $x = h$ over 21-section interdigitated channel and diffuser with permeability $k = 1.6 \times 10^{-8}$ cm^2 in the regime of full conversion of oxygen on the membrane for diffuser thickness h and inlet pressure p_1; pressure drops are (a) $\delta p = 2 \times 10^3$ Pa and (b) 2×10^4 Pa.

is the inlet pressure; p_2 is the outlet pressure; and the other notation is the same as in Eqs. 4.

Analysis of the membrane oxygen flux $\Omega_{int.dig}$, illustrated in Figure 6, shows a kind of oxygen saturation domain at high $p\Delta p$, where a further increase in the pressure gradient flow does not further increase the flux through the membrane plane. The saturated membrane oxygen flow appears to be almost independent of the number of channels. The more channels there are, the more effective the diffusion and, consequently, the higher the unsaturated flux and oxygen transport at low pressures become and the lower the pressure at which saturation occurs. For example, unsaturated membrane oxygen flux is ~ 5 times higher for a 21-channel plate than for a 6-channel plate.

The higher the permeability, the less p_1^2-p_2^2 is needed for the saturation of the diffuser by oxygen. For example, a 1-mm-thick diffuser with $k = 8\times10^{-8}\text{cm}^2$ over a 21-section interdigitated channel bed becomes saturated with oxygen for the pressures $p > 10^5$Pa, $\Delta p > 10^4$Pa.

The dependence of oxygen flow $\Omega_{int.dig}(h)$ is nontrivial (see Figure 7). High values of $p\Delta p$ and gas permeability k reduce the optimal for the oxygen transport thickness of the diffuser. For example, a diffuser with $k = 8\times10^{-8}\text{cm}^2$ over a 21-section interdigitated channel plate at $p_1 \gtrsim 10^5$Pa, $\delta p = 5\times 10^4$Pa, is mostly effective at $h \sim 100$ μm.

Serpentine (continuous channel) design

The pressure and concentration drop between two neighboring gas-supply channels constructed in PEFCs (Figure 1a) is usually rather small. Equation 7, applied to the plate of serpentine channels, gives the total flux through the membrane plane in the following form

$$\Omega_{\text{serp}} = \pi\alpha\frac{L}{h}\sum_{i=1}^{n-1}\left(\frac{E_{1i}}{H_i - G_i}\exp\frac{H_i - G_i}{2}y + \frac{E_{2i}}{H_i + G_i}\exp\frac{H_i + G_i}{2}y\right),$$

$$E_{1i} = \frac{c_{0i} - c_{1i}\exp\left\{-\dfrac{G_i + H_i}{2}d\right\}}{1 - \exp\{-G_i d\}},$$

$$E_{2i} = \frac{-c_{0i}\exp\{-G_i d\} + c_{1i}\exp\left\{-\dfrac{G_i + H_i}{2}d\right\}}{1 - \exp\{-G_i d\}}, \quad (9)$$

$$G_i = \sqrt{4F^2 + H_i^2}, \qquad F = \frac{\pi}{2h}, \qquad H_i = -\frac{\beta}{\alpha}\frac{p_{2i}^2 - p_{1i}^2}{2d},$$

where L is the length of *one section* of the serpentine channel, p_{1i}, p_{2i}, c_{0i} c_{1i} are average values of proper variables in every channel, and the other notation is the same as in (Eq. 8). In view of low pressure and concentration drops, linearization can be performed as follows:

$$p_{1i} = p_{\text{in}} + (i - 1/2)\,\delta p, \qquad \delta p = \frac{p_{\text{out}} - p_{\text{in}}}{n-1}, \qquad d = \frac{M}{(n-1)}$$

$$c_{0i} = c_{0\text{in}} + (i - 1/2)\,\delta c_0, \qquad \delta c_0 = \frac{c_{0\text{out}} - c_{0\text{in}}}{n-1},$$

$$c_{1i} = c_{0i} - \delta c_0, \quad (10)$$

where p_{out} is the outlet gas pressure; p_{in} is the inlet gas pressure; c_{0out} is the outlet reactant concentration, c_{0in} is the inlet reactant concentration; n is the number of supply channels, h is the thickness of the diffusive layer; d is the distance between the neighboring channels; and M is the width of the channel plate.

In the regime of full conversion of oxygen on the membrane, considered here, the oxygen flow Ω_{serp} over a serpentine channel with a linearized pressure and a concentration drop, behaves qualitatively similar to the oxygen flow $\Omega_{int.dig}$ over the interdigitated net. However, Ω_{serp} is due to diffusion alone in a much wider domain of low $p\Delta p$ (Figures 8 and 9). For example, in the case of a diffuser with low permeability, that is, $k = 1.6\times10^{-9}$ cm^2, $h = 250$ μm, $n = 41$, we have: Ω_{serp} is unsaturated and independent on pressure for $p < 5\times10^5$ Pa, $\Delta p < 10^5$ Pa. As the product of $p\Delta p$ increases, the saturation in the serpentine model decreases more slowly than in the interdigitated design under the same conditions (Figures 8); for example, when $n = 21$, $h = 1$ mm, $k = 8\times10^{-8}$ cm^2, Ω_{serp} becomes saturated for $p > 1.5\times10^5$ Pa, $\Delta p > 4\times10^4$ Pa. A highly permeable diffuser with $k = 8\times10^{-8}$ cm^2 over 4 1 interdigitated channels with pressures $p_1 \gtrsim 10^5$ Pa, $\delta p = 5\times10^4$ Pa provides the most effective oxygen transport when $h \sim 250$ μm.

Conclusions

The preceding results were obtained by applying the model of the gas mixture transport at nonzero pressure and concentration gradient field in porous media to oxygen transport in the porous diffusers of PEFCs. This led to the following conclusions.

The oxygen flux increases toward the catalyst layer at $x = h$, where it reaches its maximum, whereas the oxygen concentration decreases to zero. Low-pressure vlaues $p_1^2 - p_2^2$ and the gas permeability of diffuser k reduce oxygen transport, since it results from diffusion alone.

The maximum value of the catalyst oxygen flux is expressed by a transcendental function of the diffuser thickness, pressure regime, and the physical characteristics of the gases and diffuser, and is plotted as a 3-dimensional contour.

The effect of the oxygen flow saturation at high $p\Delta p$ was demonstrated, that is, a further increase in pressure and its drop does not result in increasing the oxygen flux through the membrane. The saturated flux is independent of the number of channels in the supply bed. The membrane oxygen flow Ω is independent of the permeability in the "saturation" domain, and is approximately a linear function of the diffusion coefficient, $-\Omega = \Omega(\alpha) \sim \alpha$.

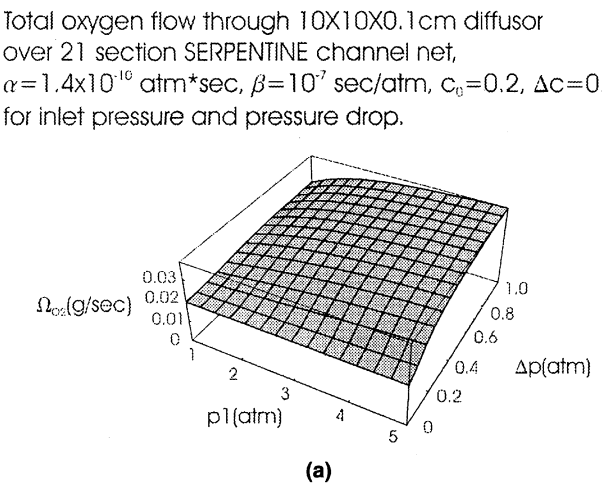

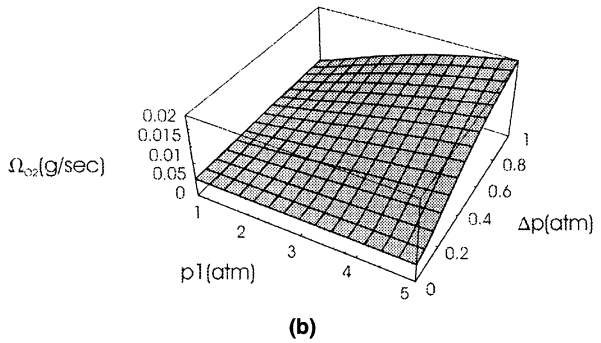

Figure 8. The oxygen flows through the membrane plane $x = h$ over 21- and 6-section serpentine channels and 1-mm-thick diffuser with permeability $k = 1.6 \times 10^{-8}$ cm^2 in the regime of full conversion of oxygen on the membrane for inlet pressure p_1 and pressure drop Δp.

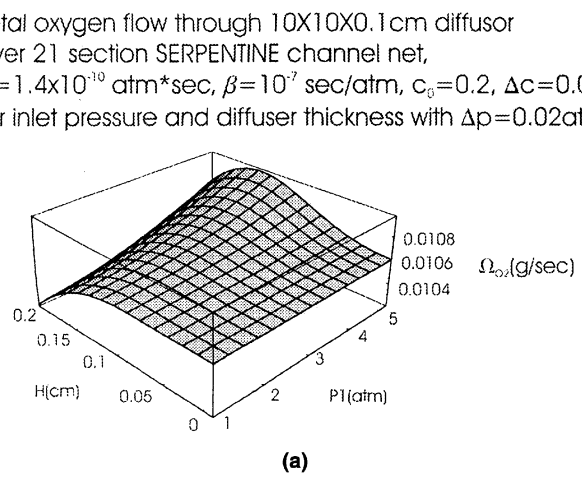

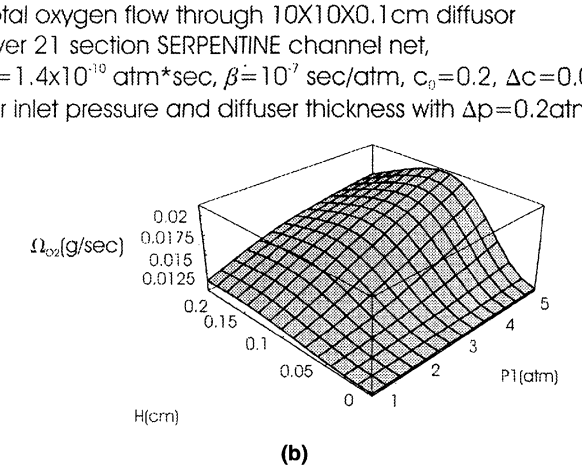

Figure 9. The oxygen flows through the membrane plane $x = h$ over 21-section serpentine channel and diffuser with permeability $k = 1.6 \times 10^{-8}$ cm^2 in the regime of full conversion of oxygen on the membrane for diffuser thickness h and inlet pressure p_1; pressure drops are (a) $\delta p = 2 \times 10^3$ Pa and (b) 2×10^4 Pa.

The saturation effect is more noticeable in materials with higher gas permeability. In the case of low permeability of a diffuser, the saturation decreases slowly, particularly for the serpentine model, compared to the interdigitated design. An increase in the unsaturated membrane oxygen flow can be achieved with a higher number of gas supply channels.

High values of $p\Delta p$ and permeability k reduce the maximum for oxygen transport diffuser thickness.

A comparison of the serpentine and interdigitated models in the full oxygen conversion regime on the membrane, considered earlier, leads to the following conclusions:

• For low values of $p\Delta p$, the serpentine model predicts the same oxygen transport rate as the interdigitated model only if the oxygen concentration remains constant along the interdigitated channels. However, in reality, oxygen depletes along interdigitated channels and its outlet concentration is low. Thus, the performance of the serpentine design appears to be higher at low pressures than that of the interdigitated design.

• For higher $p\Delta p$, the values of the oxygen flux through the membrane are somewhat lower for the serpentine model, where the saturation decreases more slowly and Ω is due to diffusion alone in a much wider $p\Delta p$ domain. However, this difference decreases with growing $p\Delta p$.

Acknowledgments

Thanks are due to Dr. L. Giorgi for fruitful conversations and discussions.

Literature Cited

Amphlett, J. C., R. M. Baumert, R. F. Mann, B. A. Peppley, P. R. Roberge, and T. J. Harris, "Performance Modeling of the Ballard

Mark IV Solid Polymer Electrolute Fuel Cell," *J. Electrochem. Soc.*, **142** (1), 1 (1995).
Bernardi, D. M., "Water Balance Calculations for Solid-Polymer-Electrolyte Fuel Cells," *J. Electrochem. Soc.*, **137**(11), 3344 (1990).
Bernardi, D. M., and M. W. Verbrugge, "Mathematical Model of a Gas Diffusion Electrode Bonded to a Polymer Electrolyte," *AIChE J.*, **37**(8), 1151 (1991).
Bernardi, D. M., and M. W. Verbrugge, "A Mathematical Model of the Solid Polymer Electrolyte Fuel Cell," *J. Electrochem. Soc.*, **139**(9), 2477 (1992).
Bird, R. B., W. E. Steward, and E. N. Lightfoot, *Transport Phenomena*, Wiley, New York (1960).
Fuller, T. F., and J. Newman, "Water and Thermal Management in Solid-Polymer-Electrolyte Fuel Cells," *J. Electrochem. Soc.*, **140**(5), 1218 (1993).
Gurau, V., F. Barbir, and H. Liu, "An Analytical Solution of a Half-Cell Model for PEM Fuel Cells," *J. Electrochem. Soc.*, **147**(7), 2468 (2000).
He, W., J. S. Yi, and T. V. Nguyen, "Two-Phase Flow Model of the Cathode of PEM Fuel Cells Using Interdigitated Flow Fields," *AIChE J.*, **46**(10), 2053 (2000).
Kumar, G. S., M. Raja, and S. Parthasarathy, "High Performance Electrodes with very low Platinum Loading for Polymer Electrolyte Fuel Cells," *Electrochim. Acta*, **40**, 285 (1995).
Nguyen, T. V., "A Gas Distribution Design for PEM Fuel Cells," *J. Electrochem Soc.*, **143**, L103 (1996).
Nguygen, T. V., and R. E. White, "A Water and Heat Management Model for PEM Fuel Cell," *J. Electrochem. Soc.*, **140**, 2178 (1993).
Perry, M. L., J. Newman, and E. J. Cairns, "Mass Transport in Gas-Diffusion Electrodes: A Diagnostic Tool for Fuel-Cell Cathodes," *J. Electrochem. Soc.*, **145**(1), 5 (1998).
Ralph, T. R., G. A. Hards, J. E. Keating, S. A. Campbell, D. P. Wilkinson, M. Davis, J. St-Pierre, and M. C. Johnson, "Low Cost Electrodes for PEM Fuel Cells," *J. Electrochem. Soc.*, **144**, 3845 (1997).
Rho, Y. W., S. Srinivasan, and Y. T. Kho, "Mass Transport Phenomena in Proton Exchange Membrane Fuel Cells Using O_2/He, O_2/Ar, and O_2/N_2 Mixtures," *J. Electrochem. Soc.*, **141**(8), 2089 (1998).
Springer, T. E., T. A. Zawodzinski, and S. Gottesfeld, "Polymer Electrolyte Fuel Cell Model," *J. Electrochem. Soc.*, **138**, 2334 (1991).
Springer, T. E., T. A. Zawodzinski, M. S. Wilson, and S. Gottesfeld, "Characterization of Polymer Electrolyte Fuel Cells Using AC Impedance Spectroscopy," *J. Electrochem. Soc.*, **143**(2), 587 (1996).
Taylor, E. J., E. B. Anderson, and N. R. K. Vilambi, "Preparation of High-Platinum-Utilization Gas Diffusion Electrodes for PEM Fuel Cells," *J. Electrochem. Soc.*, **139**, L45 (1992).
Toda, T., H. Igarashi, and M. Watanabe, "Role of Electronic Property of Pt and Pt Alloys on Electrocatalytic Reduction of Oxygen," *J. Electrochem. Soc.*, **145**(12), 4185 (1998).
Wainright, J. S., J.-T. Wang, D. Weng, R. F. Savinell, and M. Litt, "Acid Doped Polibenzimidazoles: A New Polymer Electrolyte" *J. Electrochem. Soc.*, **142**, L121 (1995).
Watanabe, M., Y. Satoh, and C. Shimura, "Management of Water Content in Polymer Electrolyte Membranes with Porous Fiber Wicks," *J. Electrochem. Soc.*, **140**(11), 3190 (1993).
White, F. M., *Viscous Fluid Flow*, McGraw-Hill, New York (1991).
Wilson, M. S., and S. Gottesfeld, "High Performance Catalyzed Membranes of Ultralow Pt Loadings for PEFC," *J. Electrochem. Soc.*, **139**, L28 (1992).
Yi, J. S., and T. V. Nguyen, "An Along the Channel Model for Proton Exchange Membrane Fuel Cells," *J. Electrochem. Soc.*, **145**, 1149 (1998).

Manuscript received Apr. 24, 2002, revision received Feb. 13, 2003, and final revision received May 19, 2003.